BOOSTED CURRICULUM REINFORCEMENT LEARNING

Anonymous authors
Paper under double-blind review

ABSTRACT

Curriculum value-based reinforcement learning (RL) solves a complex target task by reusing action-values across a tailored sequence of related tasks of increasing difficulty. However, finding an exact way of reusing action-values in this setting is still a poorly understood problem. In this paper, we introduce the concept of boosting to curriculum value-based RL, by approximating the action-value function as a sum of residuals trained on each task. This approach, which we refer to as boosted curriculum reinforcement learning (BCRL), has the benefit of naturally increasing the representativeness of the functional space by adding a new residual each time a new task is presented. This procedure allows reusing previous action-values while promoting expressiveness of the action-value function. We theoretically study BCRL as an approximate value iteration algorithm, proving its advantages over regular curriculum RL in terms of approximation accuracy and convergence to the optimal action-value function. Finally, we provide detailed empirical evidence of the benefits of BCRL in problems requiring curricula for accurate action-value estimation and targeted exploration.

1 INTRODUCTION

The combination of reinforcement learning (RL) (Sutton & Barto, 2018) algorithms with powerful function approximators, i.e., deep RL (François-Lavet et al., 2018; Mnih et al., 2015), is a major breakthrough towards solving complex decision making and control problems that were impractical for previous shallow RL methods. However, the outstanding performance of deep RL techniques is obtained at the cost of a massive amount of data needed from the interaction with the environment, hindering the practicality of deep RL methods.
Curriculum RL is a biologically inspired approach that frames the problem of learning a complex target task into learning a sequence of simplified, increasingly difficult, versions of it (Florensa et al., 2017; Shao et al., 2018; Ivanovic et al., 2019; Narvekar et al., 2020). Commonly, establishing the complexity of a task in RL is not trivial, as an indisputable notion of complexity is still missing. However, from a practical point of view, we can consider a task complex if it requires targeted exploration in the environment or complex policies to be solved. In curriculum RL, the notion of task complexity is key, and it is assumed that tailored tasks in a sequence of increasing complexity are presented to the learning agent. Such an appropriate design is, however, a difficult problem, requiring either human expertise (Narvekar et al., 2020) or solutions to automatize the selection of tasks following the learning of the agent (Jiang et al., 2015; Svetlik et al., 2017; Klink et al., 2020). Regardless of using a handcrafted or an automatically generated curriculum, a common approach adopted by most value-based curriculum RL methods is to use the same function approximator throughout all the tasks (Narvekar et al., 2020): given a task, an approximation of the action-value function is learned, and used as an initialization for learning the action-value function of the next task in the curriculum. For the success of this procedure, the function approximator needs to be powerful enough to handle the complexity of the target task. However, this requirement raises the key issue of adequately designing the function approximator. A complex function approximator is prone to overfitting, and sensitive to hyper-parameters, being detrimental for learning simple tasks in the curriculum; conversely, using an overly simple function approximator can hinder the learning of the target task. Moreover, choosing an adequate function approximator *a-priori* is not trivial, as the target task is only visited at the end, and it is commonly unsolvable by non-curriculum RL methods.

In this paper, we introduce a novel approach that models the action-value function of a task as a sum of residuals learned on the previous tasks in the curriculum. Our method increases the representativeness of the function approximator as new tasks are presented to the agent, leading to a procedure

that increases the size of the functional space as the curriculum proceeds. This results in a learning procedure that increases the power of the function approximator according to the complexity of the task at hand, using small models in simple problems to avoid overfitting, and using large models (resulting from the sum of small ones) to handle the dimensionality of complex problems. Notably, if the curriculum is sufficiently fine-grained, the residuals become smoother functions, close to zero, that are easy to learn, even if the respective tasks are harder than the previous ones. We call our method boosted curriculum reinforcement learning (BCRL), for its resemblance with the boosting technique in supervised learning (Freund, 1995). We provide a theoretical analysis of our approach under the lens of the approximate value iteration (AVI) framework (Farahmand, 2011). In AVI, an estimate of the optimal action-value function is obtained as an iterative process that starts from an arbitrary estimate and applies the optimal Bellman operator until convergence. It is shown that two sources of error exist in AVI: (i) computation of the optimal Bellman operator, (ii) representation of the action-value function (Farahmand, 2011). While the former is due to the need of using samples to approximate the unknown optimal Bellman operator, the latter depends on the representativeness of the functional space chosen to approximate the action-value function. In this work, we formalize the curriculum RL problem in the AVI setting to show that the representation of the action-value function obtained by BCRL results in a tighter bound on the approximation error compared to regular curriculum RL, consequently reducing the performance loss. We complement this analysis with an empirical evaluation of BCRL in AVI and RL settings, resorting to the fitted Q-iteration (FQI) algorithm (Ernst et al., 2005), least-squares policy iteration (LSPI) (Lagoudakis & Parr, 2003) and deep Q-networks (Mnih et al., 2015), where we confirm the advantages of BCRL over regular curriculum RL and a related baseline (Tosatto et al., 2017).

2 Related work

Learning under a dynamic set of training experience has been investigated in different fields throughout decades (Saul, 1941; Elman, 1993; Asada et al., 1996; Krueger & Dayan, 2009). A recent paper by Bengio et al. (2009) has established the term *curriculum learning* for the concept of organizing training data of a neural network in a beneficial way for performance and generalization. This term carried over to the domain of RL, where curricula over training tasks have been shown to stabilize the highly challenging optimization problem of RL (Narvekar et al., 2020). While a large body of research in the domain of curriculum reinforcement learning investigates the interesting problem of optimally selecting and scheduling the training tasks for an RL agent to optimize performance on a set of target tasks (Florensa et al., 2017; Ivanovic et al., 2019; Shao et al., 2018; Klink et al., 2020), the architecture of the learning agent is assumed fixed and the transfer of agent behavior between subsequent tasks in the curriculum is realized by this shared fixed architecture.
However, aside from investigations into the benefit of an adequately chosen evolution of training experience, investigations of an optimal learning architecture (Elsken et al., 2019) and the evolution of this architecture during learning (Aoki & Siekevitz, 1988; Rumelhart et al., 1988; Ash, 1989; Fahlman, 1990; Lahnajärvi et al., 2002; Nitanda & Suzuki, 2018) have been conducted in supervised learning scenarios. The adaptation of these methods to the setting of RL has been limited to on-policy temporal-difference learning (Rivest & Precup, 2003; Vamplew & Ollington, 2005b;a) and it has not been further pursued in recent years. Our work aims to improve the information transfer between subsequent tasks in curriculum value-based reinforcement learning via a boosting procedure (Freund, 1995). The benefit of the boosting framework is that it is well understood from a theoretical perspective (Tosatto et al., 2017), allowing for the derivation of error bounds, as also presented in this paper. Further, it is agnostic to any value-based RL algorithm, avoiding the need to adjust the RL algorithm of choice to be suited for the evolution of the function approximator (Rivest & Precup, 2003; Vamplew & Ollington, 2005a;b).

3 Preliminaries

3.1 Definitions and notation

We recall the notions about Markov Decision Processes (MDPs) (Puterman, 1990), and the notation used for approximate value iteration (AVI) (Farahmand, 2011), that are relevant to our work.

For a space Σ, we define $\mathcal{M}(\Sigma)$ the set of probability measures over the σ-algebra σ_Σ. We denote $\mathcal{B}(\Sigma, B)$ as the space of bounded measurable functions w.r.t. σ_Σ with bound $0<B<\infty$. A finite-action discounted MDP is defined as a tuple $\mathcal{T} = \langle \mathcal{S}, \mathcal{A}, \mathcal{P}, \mathcal{R}, \gamma \rangle$, where $\mathcal{S}$ is a measurable state space, $\mathcal{A}$ is a finite set of actions, $\mathcal{P} : \mathcal{S} \times \mathcal{A} \to \mathcal{M}(\mathcal{S})$ is a transition kernel, $\mathcal{R} : \mathcal{S} \times \mathcal{A} \times \mathcal{S} \to \mathbb{R}$ is a reward function, and $\gamma \in [0, 1)$ is a discount factor. A policy π is a mapping from the state space $\mathcal{S}$ to a probability distribution over the action space $\mathcal{A}$. A policy induces an action-value function $Q^\pi(s, a) \triangleq \mathbb{E}\left[\Sigma_{t=0}^{\infty} \gamma^t R_t | S_0{=}s, A_0{=}a\right]$, corresponding to the expected cumulative discounted reward obtained performing action a in state s and following the policy π thereafter. RL aims at solving an MDP by finding an optimal policy π^* which induces an optimal action-value function $Q^*(s, a) = \sup_\pi Q^\pi(s, a)$. For immediate rewards uniformly bounded by $R_{\max}$, the action-value function is bounded by $Q_{\max} = {}^{R_{\max}}/_{1-\gamma}$. For a probability measure $\mu \in \mathcal{M}(\mathcal{S} \times \mathcal{A})$, we define the $L_p(\mu)$-norm of a measurable function $Q \in \mathcal{B}(\mathcal{S} \times \mathcal{A})$ as $\|Q\|_{p,\mu} \triangleq [\int_{\mathcal{S}\times\mathcal{A}} |Q(s, a)|^p d\mu(s, a)]^{1/p}$. Given a sequence of values $x_{1:n}{=}(x_1, \ldots, x_n)$ for some space $\mathcal{X}$, the empirical L_p-norm of a function $f : \mathcal{X} \to \mathbb{R}$ is $\|f\|_{p,x_{1:n}} \triangleq \frac{1}{n} \sum_{i=1}^{n} |f(x_i)|^p$. Conveniently, when $X_i \sim \mu$, we have $\mathbb{E}\left[\|f\|_{p,x_{1:n}}\right] = \|f\|_{p,\mu}$. From now on, we consider the L_2-norm when the subscript p is omitted.

Operators. We define the operator P^π as $(P^\pi Q)(s, a) \triangleq \int_{\mathcal{S}} \mathcal{P}(ds'|s, a) \sum_{a' \in \mathcal{A}} \pi(a'|s') Q(s', a')$, for any given policy π. Then, the Bellman operator $T^\pi : \mathcal{B}(\mathcal{S} \times \mathcal{A}) \to \mathcal{B}(\mathcal{S} \times \mathcal{A})$ is $(T^\pi Q)(s, a) \triangleq r(s, a) + \gamma(P^\pi Q)(s, a)$. The optimal Bellman operator $T^* : \mathcal{B}(\mathcal{S} \times \mathcal{A}) \to \mathcal{B}(\mathcal{S} \times \mathcal{A})$ is $(T^* Q)(s, a) \triangleq r(s, a) + \gamma \int_{\mathcal{S}} \max_{a'} \mathcal{P}(ds'|s, a) Q(s', a'))$. Finally, the fixed point of the Bellman operator is $(T^\pi Q^\pi) = Q^\pi$, and the fixed point of the optimal Bellman operator is $(T^* Q^*) = Q^*$. As in Györfi et al. (2006), we define the truncation operator $\beta_B : \mathcal{B}(\mathcal{S} \times \mathcal{A}) \to \mathcal{B}(\mathcal{S} \times \mathcal{A}, B)$ such that, given a function $f \in \mathcal{B}(\mathcal{S} \times \mathcal{A})$, we have $\beta_B f(s, a) \in [-B, B], \forall (s, a) \in \mathcal{S} \times \mathcal{A}$.

3.2 Approximate value iteration

The family of approximate value iteration (AVI) algorithms (Sutton & Barto, 2018; Farahmand, 2011; Munos, 2005) aims at approximating the solution of RL problems with large state space where finding an optimal solution is impractical or impossible. Starting from an arbitrary estimate Q^0, AVI algorithms iteratively approximate the application of the optimal Bellman operator in a suitable functional space, i.e., $Q^{k+1} \approx T^* Q^k$. Intuitively, the approximation error at each iteration plays a central role in terms of convergence to the fixed point Q^*. The approximation error results from two key aspects: (i) the unknown optimal Bellman operator, and (ii) the representation of the action-value function in a suitable functional space $\mathcal{F}$ via the application of a nonlinear operator $S : \mathcal{B}(\mathcal{S} \times \mathcal{A}) \to \mathcal{F}$ defined as $Sy = \arg\inf_{f \in \mathcal{F}} \|f - y\|_\mu^2$ for any $y \in \mathcal{B}(\mathcal{S} \times \mathcal{A})$. We denote the resulting approximation error by

$$\varepsilon_k \triangleq T^* Q^k - Q^{k+1}. \tag{1}$$

The role of the approximation error in AVI is evinced by the following theorem that bounds the performance loss, w.r.t. the optimal performance, at iteration K[1].

Theorem 1. *((Farahmand, 2011)). Let K be a positive integer, ρ an initial state distribution, and $Q_{max} \leq \frac{R_{max}}{1-\gamma}$. Then, for any sequence $(Q_k)_{k=0}^K \subset B(\mathcal{X} \times \mathcal{A}, Q_{max})$, and the corresponding sequence $(\varepsilon_k)_{k=0}^{K-1}$ defined in (1), we have*

$$\|Q^* - Q^K\|_{1,\rho} \leq \frac{2\gamma}{(1-\gamma)^2} \left[\inf_{r \in [0,1]} C_{VI,\rho,\mu}^{\frac{1}{2}}(K; r) \mathcal{E}^{\frac{1}{2}}(\varepsilon_0, \ldots, \varepsilon_{K-1}; r) + \frac{2}{1-\gamma} \gamma^K R_{max} \right]$$

where

$$C_{VI,\rho,\mu}(K; r) = \left(\frac{1-\gamma}{2}\right)^2 \sup_{\pi'_1, \ldots, \pi'_K} \sum_{k=0}^{K-1} \alpha_k^{2(1-r)} \left[\sum_{m \geq 0} \gamma^m \Big(c_{VI_1,\rho,\mu}(m, K-k; \pi'_K) + c_{VI_2,\rho,\nu}(m+1; \pi'_{k+1}, \ldots, \pi'_K) \Big) \right]^2$$

and $\mathcal{E}(\varepsilon_0, \ldots, \varepsilon_{K-1}; r) = \sum_{k=0}^{K-1} \alpha_k^{2r} \|\varepsilon_k\|_\mu^2$.

We refer to Farahmand (2011) for the definition of c_{VI_1}, c_{VI_2}, and α_i.

[1] In Farahmand (2011), the action-value function at iteration k is denoted by Q^{π_k} to highlight its dependency on the policy π_k. In this paper, we simply write Q^k omitting π for simplicity.

4 CURRICULUM REINFORCEMENT LEARNING WITH BELLMAN RESIDUALS

We consider the classic curriculum RL scenario where an agent aims at learning a complex target task by solving a predefined sequence of easier, but increasingly challenging, versions of it (Narvekar et al., 2020). To avoid confusion on the debatable notion of difficulty of a task, in this work we adopt a practical point of view where the difficulty of a task is related to well-known aspects of RL, e.g., the complexity of the policies for solving them and challenging exploration (Florensa et al., 2017; Ivanovic et al., 2019; Klink et al., 2020).

4.1 APPROXIMATE VALUE ITERATION IN CURRICULUM REINFORCEMENT LEARNING

Let $\mathcal{T}_{1:n} = \{\mathcal{T}_1, \dots, \mathcal{T}_n\}$ be a sequence of increasingly complex MDPs sharing the same state and action spaces, i.e., $\mathcal{T}_i = \langle \mathcal{S}, \mathcal{A}, \mathcal{P}_i, \mathcal{R}_i, \gamma \rangle$, and $\mathcal{T}_n$ be the target task. The use of AVI algorithms in this curriculum RL setting consists in starting from an arbitrary estimate Q_1^0 (where the subscript indicates the position of the task in the curriculum) and approximating the application of the task-specific optimal Bellman operator for the current task $Q_t^{k+1} \approx T_t^* Q_t^k$, or when the task at hand changes $Q_{t+1}^{k+1} \approx T_{t+1}^* Q_t^k$. We assume that the task changes when the estimate of the action-value of the current task converges. For simplicity, and without loss of generality, we denote K_t the number of iterations needed to converge for each task $\mathcal{T}_t$, and denote $Q_t^0 = Q_{t-1}^{K_{t-1}} = Q_{t-1}^*$.

Lemma 1. *Let K be the current iteration. Then,*

$$\|Q_n^* - Q_t^K\|_{1,\rho} \leq \|Q_n^* - Q_n^0\|_{1,\rho} + \dots + \|Q_t^* - Q_t^K\|_{1,\rho} = \sum_{i=t+1}^{n} \|Q_i^* - Q_i^0\|_{1,\rho} + \|Q_t^* - Q_t^K\|_{1,\rho}. \quad (2)$$

This result can be verified applying the triangle inequality under the assumption that the algorithm switches task when the stopping condition of the algorithm is verified, e.g., when reaching a chosen number of iterations K_t that allows the action-value function estimate to converge, or using heuristic methods checking the magnitude of the update (Lagoudakis & Parr, 2003; Ernst et al., 2005). Note that each component of the sum in (2) can be bounded by the result in Theorem 1. We denote the k-step Bellman residual for task t by

$$\varrho_t^k \triangleq (T_t^*)^k Q_{t-1}^* - Q_{t-1}^* = (T_t^*)^k Q_t^0 - Q_t^0. \quad (3)$$

Proposition 1. *Given an initial $Q_1^0(s,a)$=0 for any $(s,a) \in \mathcal{S} \times \mathcal{A}$, and considering that $Q_t^* = Q_t^{K_t} \approx (T_t^*)^{K_t} Q_{t-1}^*$, we obtain*

$$\varrho_n^k + \sum_{t=1}^{n-1} \varrho_t^{K_t} = (T_n^*)^k Q_n^0 - Q_n^0 + \left(\sum_{t=1}^{n-1} (T_t^*)^{K_t} Q_t^0 - Q_t^0 \right) = (T_t^*)^k \dots (T_1^*)^{K_1} Q_1^0 - Q_1^0 \approx Q_n^k. \quad (4)$$

This result shows that, approximately, the action-value function of the target task is equivalent to the sum of k-step Bellman residuals. Notably, especially if the curriculum is sufficiently fine-grained, residuals becomes progressively smoother and smaller. In the following, we describe how to compute the estimate shown in (4).

4.2 BOOSTED CURRICULUM REINFORCEMENT LEARNING

It is well-known from supervised learning that: (i) small function approximators are easier to train, and thus are desirable to solve simple tasks; (ii) large function approximators can overfit or suffer slow training speed in simple tasks, but they are more suitable to handle complex problems. Ideally, we want to increase the representativeness of the function approximator with the increase of task complexity. Recalling (4), we propose to use a separate function approximator for each residual ϱ_t, i.e. a separate approximator for each task. Given a dataset $\mathcal{D}_t = \{(s_t^i, a_t^i, r_t^i, s_t'^i)\}_{i=1}^N$ for each task, we denote the empirical Bellman operator by $(\hat{T}_t^* Q)(s_t^i, a_t^i) \triangleq r_t^i + \gamma \max_{a'} Q(s_t'^i, a')$, and define the k-step empirical residual as $\tilde{\varrho}_t^k \triangleq (\hat{T}_t^*)^k Q_t^0 - Q_t^0$. At iteration k, for a current task t, and defining the nonlinear operator $\hat{S}$ as the empirical version of the operator S, we compute an approximation

$$Q_t^k = Q_t^0 + \beta_{B_k} \hat{S} \tilde{\varrho}_t^k = \sum_{i=1}^{t-1} \hat{\varrho}_i^{K_i} + \hat{\varrho}_t^k, \quad (5)$$

Algorithm 1: Boosted Curriculum Reinforcement Learning (BCRL)

Input: Tasks $\mathcal{T}_{1:n}$, $t = 1$, dataset $\mathcal{D}$, $Q_1^0 = 0$;
while $t < n + 1$ **do**
  for $k = 0, \dots, K_t$ **do**
    $\tilde{\varrho}_t^k \leftarrow \hat{T}_t^* Q_t^k - Q_t^0$;
    $Q_t^{k+1} \leftarrow Q_t^0 + \beta_{B_k} \arg\inf_{f \in \mathcal{F}} \| f - \tilde{\varrho}_t^k \|_\mu$;
  end
  $Q_{t+1}^0 \leftarrow Q_t^{K_t}$;
  $t \leftarrow t + 1$;
end
Output: $Q_n^{K_n} = \sum_{t=1}^n \hat{\varrho}_t^{K_t}$.

where we defined $\hat{\varrho}_t^k = \beta_{B_k} \hat{S} \tilde{\varrho}_t^k$ for compactness. We call this approach *boosted curriculum reinforcement learning* (BCRL), for its resemblance with the boosting procedure in supervised learning (Schapire, 1990; Freund, 1995), and we show its pseudocode in Algorithm 1.

Remarks. Our approach is based on the key insight that the strength of the function approximator should increase according to the complexity of the task at hand. In BCRL, we accomplish this estimating an action-value function through a sum of action-value functions of the previous tasks in the curriculum. Thus, contrary to methods using the same functional space for all tasks, our approach has the advantage of acting in an augmented functional space resulting from the sum of the functional space of each approximator. In supervised learning literature, the function approximators in the sum are commonly known as weak regressors, meaning that boosting has the advantage of estimating complex functions as a sum of simple regressors (Geurts et al., 2006). Similarly, our BCRL procedure can use simple function approximators for each task in the curriculum, with the advantages that (i) easy tasks can be learned with easy function approximators curbing the risk of overfitting, (ii) the complexity of the function approximator can be chosen according to the first tasks in the curriculum, contrarily to regular curriculum RL where the function approximator needs to be suitable for the target task, and (iii) the training time to fit the model on each task is reduced due to the smoothness of the residuals. Conversely, at inference time, our method requires a forward pass for each approximator in the ensemble. Nevertheless, the small size of the regressors results in negligible increase of computation time. Finally, we clarify that the soundness of this procedure is guaranteed by the fact that if the functional space of each weak regressor is Glivenko-Cantelli, i.e., "the error due to the empirical process goes to zero at least asymptotically", then, due to the preservation theorem, also the space resulting from the sum of weak regressors is Glivenko-Cantelli (Van Der Vaart & Wellner, 2000; Tosatto et al., 2017).

5 Theoretical Analysis

In this section, we provide a theoretical analysis of BCRL in terms of convergence guarantees and finite-sample approximation error analysis. For simplicity and ease of notation, we assume the tasks in the curriculum have the same transition kernels, and different reward functions. Nevertheless, our results can be straightforwardly extended to the general case. We refer to the well-known results in AVI (Farahmand, 2011; Farahmand et al., 2010), and the analysis provided in Tosatto et al. (2017), with which our analysis share some similarities.

5.1 Convergence Guarantees

Theorem 2. *Let Q_{t-1}^* be the learned action-value for task $\mathcal{T}_{t-1}$, and $(Q_t^i)_{i=0}^k$ be a sequence of measurable action-value functions for a target task $\mathcal{T}_t$ obtained following our* BCRL *procedure (5), where $Q_t^0 = Q_{t-1}^*$. Denote $L = \gamma C_{\mu \to \infty}$ the Lipschitz coefficient of the optimal Bellman operator, where $C_{\mu \to \infty}$ is the one-step concentrability coefficient w.r.t. μ (Farahmand, 2011), and assume the operator S is such that $\exists \lambda > 0 : \|(I - S)y\|_\mu \leq \lambda \|y\|_\mu$ for all $y \in \mathcal{B}(\mathcal{S} \times \mathcal{A})$. Then,*

$$\|Q_t^k - Q_t^*\|_\mu \leq ((1 + L^k)\lambda + L^k) \|Q_t^0 - Q_t^*\|_\mu. \tag{6}$$

We observe that the boosting procedure adds the $(1 + L^k)\lambda$ term in the regular AVI bound, that is obtained for $\lambda = 0$. This result shows that for each task, for appropriate values of λ and L, the boosting procedure converges to the optimal action-value.

Corollary 1. *Given the settings of Theorem 2, the sequence of $(Q_t^i)_{i=0}^k$ converges to Q_t^* when*

$$\lambda < \frac{1 - L^k}{1 + L^k} \quad \textit{and} \quad L^k < 1. \tag{7}$$

5.2 Finite-sample approximation error analysis

In Lemma 1, we show how to derive the AVI performance loss analysis (Farahmand, 2011) for curriculum RL. Now, we want to characterize it for our BCRL method. Instead of using the regular AVI approximation error defined in (1), we consider the approximation error for each task t in the curriculum defined as

$$\varepsilon_t^k = (T_t^*)^k Q_t^0 - Q_t^k \quad , \quad \varepsilon_t^0 = (T_{t-1}^*)^{K_{t-1}} Q_{t-1}^0 - Q_t^0. \tag{8}$$

Theorem 3. *Let $(Q_t^i)_{i=0}^k$ be a sequence of action-value function for each task t, $(\varepsilon_t^i)_{i=0}^k$ be the respective sequence of approximation errors as defined in (8), $\mathcal{F} \subseteq \mathcal{B}(\mathcal{S} \times \mathcal{A})$ be a subset of measurable action-value functions. Denoting the regular AVI residual as $\bar{\varrho}_t^k = (T_t^*)^k \dots (T_1^*)^{K_1} Q_1^0 - (T_{t-1}^*)^{K_{t-1}} \dots (T_1^*)^{K_1} Q_1^0$, we have*

$$\inf_{f \in \mathcal{F}} \|f - \varrho_t^k\|_\mu \leq \inf_{f \in \mathcal{F}} \|f - \bar{\varrho}_t^k\|_\mu + (1 + L^k)\Big(\sum_{i=1}^{t-1} L^{K_i} \|\varepsilon_i^0\|_\mu + \|\varepsilon_t^0\|_\mu\Big). \tag{9}$$

This bound shows the relation between the approximation error of the residual for task t at step k, the AVI Bellman Residual $\bar{\varrho}_t^k$, and the approximation error for the residuals of the previous tasks.

Lemma 2. *Let $(Q_t^i)_{i=0}^k$ be a sequence of action-value function for each task t, $(\varepsilon_t^i)_{i=0}^k$ be the respective sequence of approximation errors as defined in (8). Then,*

$$\|\tilde{\varrho}_t^k\|_\infty \leq \sum_{i=1}^{k-1} \gamma^{k-i} \|\varepsilon_t^i\|_\infty + (1 + \gamma^k) R_t^{\max}. \tag{10}$$

We use (9) and (10) to finally bound the approximation error of the residual as follows.

Theorem 4. *Let $B_k^t = \max(\|\tilde{\varrho}_t^k\|_\infty, 1)$, and $V_{\mathcal{F}^+}$ be the VC-dimension of $\mathcal{F}^+$, which is the class of all subgraphs of functions $f \in \mathcal{F}$ (Györfi et al., 2006). For given dataset $\mathcal{D}_t = \{(s_t^i, a_t^i, r_t^i, s_t'^i)\}_{i=1}^N$ for each task t, and a given sequence of action-value functions $(Q_t^i)_{i=0}^k$ generated by our* BCRL*, we have*

$$\begin{aligned} \|\varepsilon_t^k\|_\mu^2 \leq\ & 2 \inf_{f \in \mathcal{F}} \|f - \bar{\varrho}_t^k\|_\mu^2 + 2(1 + L^k)^2 \Big(\sum_{i=1}^{t-1} L^{k_i} \|\varepsilon_i^0\|_\mu + \|\varepsilon_t^0\|_\mu\Big)^2 \\ & + \frac{5136 B_t^{k^4}}{N} \Big(\log 42e + 2\log(480 e B_t^{k^2} N) V_{\mathcal{F}^+}\Big). \end{aligned} \tag{11}$$

This result bounds the error of BCRL by a sum of three components: (i) the approximation error of the residual $\bar{\varrho}_t^k$, (ii) the propagation error due to approximation errors at previous iterations, (iii) the estimation error due to the regression problem with finite amount of samples. The advantages of BCRL are motivated by the use of residuals $\bar{\varrho}_t^k$ and $\tilde{\varrho}_t^k$, whose range of values become smaller as the curriculum proceeds, resulting in tighter approximation and estimation error bounds compared to regular curriculum RL. Moreover, BCRL enjoys advantages in terms of sample-efficiency, as fewer samples than regular curriculum RL can be used to achieve comparable estimation errors, due to the smaller range and smoother shape of the target $\|\tilde{\varrho}_t^k\|_\mu$ compared to $Q_t^{\max}$.

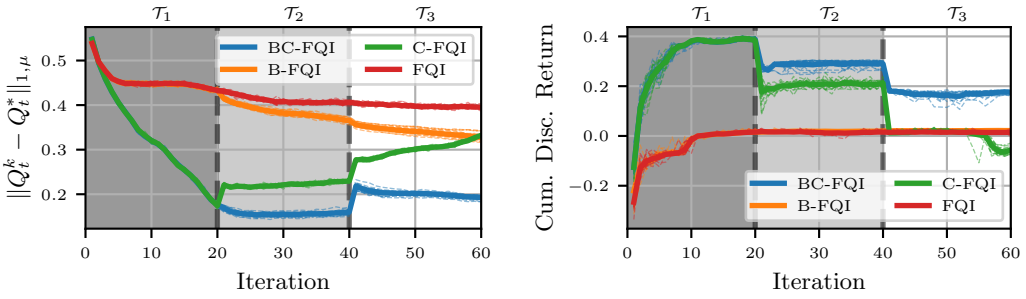

Figure 1: Mean absolute error (solid, bold lines) and standard error of the approximated Q_t-function over iterations as well as the corresponding performance obtained from a greedy policy w.r.t. this Q_t-function in task $\mathcal{T}_t$ in the car-on-hill environment (computed from 20 seeds). The differently shaded areas highlight the iterations on which BC-FQI and C-FQI trained on tasks $\mathcal{T}_1$, $\mathcal{T}_2$ and $\mathcal{T}_3$. The fine, dashed lines indicate the results of the individual 20 runs from which the mean was computed.

6 Experiments

This section serves to provide empirical evidence to the insights obtained in the previous section. More precisely, we want to provide evidence that boosted curricula can indeed improve the residual in an AVI setting and with that improve the achieved agent performance. Further, we show that the additional flexibility of boosting w.r.t. the individual function approximators can be leveraged to choose the best-suited learning approach for each learning task.

We conduct experiments in multiple environments and with two different RL algorithms using the MushroomRL library (D'Eramo et al., 2021).[2] To evaluate the benefit of curricula in boosted AVI settings, we turn towards the fitted Q-iteration (FQI) algorithm in the car-on-hill environment (Ernst et al., 2005), as the low-dimensionality allows for uniform sampling of the state-action space assumed in the previous section and the ground truth optimal Q-function can be computed via brute-force methods (Ernst et al., 2005). Next, we evaluate the FQI algorithm in a maze environment in which exploration is guided by the currently estimated optimal policy. Finally, we investigate boosting in a control task with DQN (Mnih et al., 2015), in which a point-mass needs to be steered over a narrow pathway subject to external perturbations. To disentangle the interplay between boosting and the use of a curriculum, we will compare different methods in the experiments: the algorithm under investigation (FQI, DQN), a version using both a curriculum with boosting (BC-FQI, BC-DQN) as well as two ablations of the second method - one without boosting (C-FQI, C-DQN) and one without a curriculum (B-FQI, B-DQN). The boosted methods that do not use a curriculum will introduce the additional approximators at the same iteration at which the curricula switches between tasks.

6.1 Car-on-hill

The three car-on-hill tasks $\mathcal{T}_1$, $\mathcal{T}_2$ and $\mathcal{T}_3$ considered for curriculum learning in this experiment differ in the mass of the car, taking values of 0.8, 1.0 and 1.2 respectively. The default mass of the environment is 1.0 which means we are considering a version of this environment with more challenging exploration, as the car needs more energy to escape the valley and receive a reward signal. The dataset for learning the Q-function in each task is generated by executing 1000 trajectories with a random policy. To not make the results in this section dependent on the parametric form of the function approximator, we resort to the tree-based regression investigated in Ernst et al. (2005). The results are visualized in Figure 1. We can see that the combination of boosting and a curriculum (BC-FQI) outperforms all other methods both in terms of final approximation error achieved on $\mathcal{T}_3$ but also in terms of the performance of the greedy policy derived from the estimated Q-function. Comparing the residual of BC-FQI and C-FQI, we can see that C-FQI seems to be challenged with adapting the Q-function from $\mathcal{T}_1$ to $\mathcal{T}_2$, as the jump in residual shows. BC-FQI does not exhibit such a jump in residual when moving from $\mathcal{T}_1$ to $\mathcal{T}_2$. Furthermore, BC-FQI reduces the increased residual after switching from $\mathcal{T}_2$ to $\mathcal{T}_3$ while the residual of C-FQI steadily increases once arriving at the target task. We can particularly see that the pre-training in $\mathcal{T}_1$ and $\mathcal{T}_2$ leads to a significantly smaller

[2]Code for reproducing the results is contained in the supplementary material and will be made available upon acceptance. Additional experimental details can be found in the appendix.

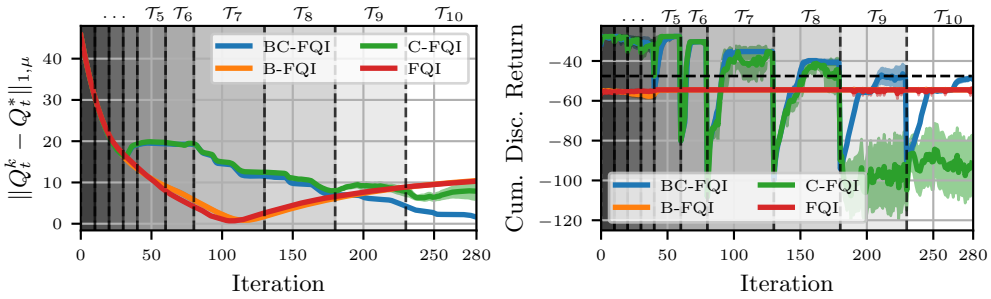

Figure 2: Average error in the approximated Q_t-functions plus corresponding performance obtained from a greedy policy w.r.t. this Q_t-function in the maze environment. Shaded colored areas correspond to two times standard error estimated from 40 seeds. The different shades of grey highlight the iterations in which BC-FQI and C-FQI trained on different tasks $\mathcal{T}_t$. The horizontal black dashed line in the right plot highlights the maximum achievable reward in $\mathcal{T}_{10}$.

Q-function error of BC-FQI compared B-FQI at iteration 40, which is in line with the discussion in the previous sections.

6.2 MAZE

We design a maze environment, in which an agent needs to reach a target position by navigating around two large obstacles. To reach the goal, the agent can choose between 4 discrete actions that move the agent up, down, left, or right. It obtains a dense reward based on the distance to the target and a reward of $+5$ upon reaching the goal. We design a curriculum composed of 10 tasks, in which the size of the walls gradually increases (see Figure 3a for a visualization of tasks contained in the curriculum). The reward function and the target task are designed to induce highly challenging exploration, requiring the use of curricula to solve the problem. As done for the car-on-hill experiment, we use FQI with tree-based regression (Ernst et al., 2005). For all methods, we collect a dataset for each task running 500 episodes using ε-greedy exploration, decreasing the strength of exploration as the curriculum proceeds. As can be seen in Figures 2 and 3, regular learning on the target task does not allow find a good solution, regardless of whether boosting is used or not (B-FQI and FQI). This is due to the highly challenging exploration problem that needs to be solved in this environment. The initial random exploration is insufficient to maneuver around the second wall in the target task. Consequently, the agent is not aware of the benefit of this detour, as obvious in the learned Q-function (Figure 3b). Subsequently reducing the exploration does not lead to any new evidence and hence the agent quickly converges to the sub-optimal solution (Figure 2). Looking at the results of C-FQI, we see that the curriculum alleviates the aforementioned exploration problem. However, the estimated Q-function deteriorates before approaching the target task, leading to unreliable policies. By introducing additional capacity as learning proceeds, BC-FQI allows to learn an optimal policy. Indeed, we show in the appendix that the residuals of BC-FQI decrease in later iterations, easing the function approximation problem when progressing to the target task.

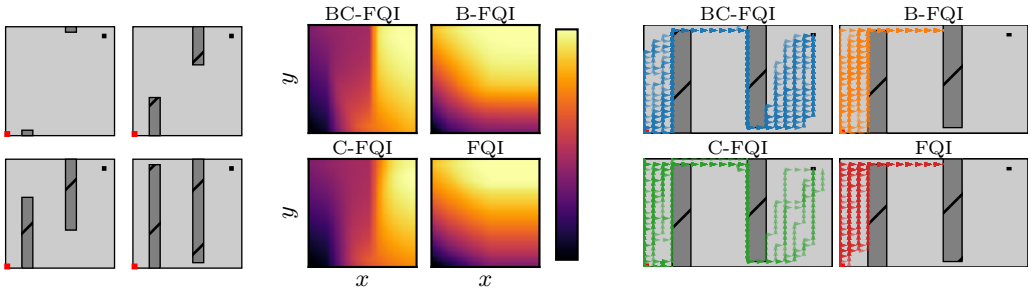

(a) Maze Environments (b) Estimated Q-function in $\mathcal{T}_{10}$ (c) Generated trajectories using Q_{10}

Figure 3: (a) visualizes different maze environments $\mathcal{T}_1$, $\mathcal{T}_4$, $\mathcal{T}_7$ and $\mathcal{T}_{10}$ (left to right, top to bottom). (b) shows the final Q-functions on $\mathcal{T}_{10}$ estimated by the evaluated approaches. (c) visualizes the trajectories generated by the corresponding agents.

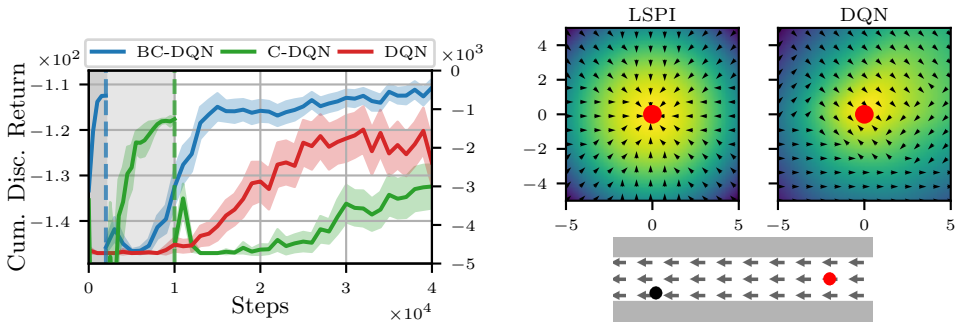

(a) Agent Performance

(b) Learned LQR Q-Functions and Target Env.

Figure 4: (a) shows the mean performance and standard error in the linear system control task achieved with different methods. The vertical dashed lines indicate the iterations at which BC-DQN and C-DQN switch from the LQR task to the target task. Statistics have been computed from 80 seeds. (b) visualizes the Q-functions learned during the pre-training in the LQR task with LSPI (for BC-DQN) and DQN (for C-DQN). The arrows indicate the policy encoded by the Q-functions.

6.3 Linear system control

The last task aims at highlighting a more subtle benefit of BCRL: Choosing the architecture of the function approximators appropriately for each task in the curriculum. We show that this flexibility can improve sample efficiency in a control task, in which a point mass needs to be steered towards a goal position over a narrow pathway (Figure 4b). Along this pathway, the point mass is subject to a drift moving it away from the target position. If the agent falls off the pathway, it is reset to the initial position. The agent receives a reward of -1 until reaching the goal. Upon reaching the goal, a reward of 0 is achieved and the episode terminates. We learn a policy for solving this target task using DQN. We introduce a curriculum for learning this task by first training in an LQR system to induce a bias of moving towards the target. In this LQR system, the point mass behaves according to the same dynamics as in the target environment and needs to reach the same target position, but does not face any external perturbations, obtains a reward equal to the negative squared distance to the target position and does not need to stay on a particular pathway. A benefit of environments with the aforementioned characteristics is that the Q-function can be shown to be a quadratic function of action and state (Bradtke, 1993). Since the boosting framework does not prescribe the architecture of the individual employed function approximators, we can exploit the aforementioned structure of the first (LQR) learning task by employing least-squares policy iteration (LSPI) (Lagoudakis & Parr, 2003) with quadratic features.

Figure 4a shows that this incorporation of additional structure into the curriculum leads to improved performance over both directly learning on the target task (DQN) and not adjusting the structure of the agent to the learning task in the curriculum (C-DQN). It is particularly surprising that C-DQN is performing even worse than DQN. There are multiple potential causes for this poor performance. One is that the DQN algorithm takes significantly longer to learn in the LQR task compared to LSPI (10.000 vs. 2.000 steps). Further, the learned Q-function and policy is not as accurate as the one learned with LSPI, as can be seen in Figure 4b. Consequently, the policy is not as stable. Finally, due to the different reward structures of the two learning tasks, the Q-function needs to adjust during learning on the target task, potentially unlearning the stabilizing behavior induced by the initial task. BC-DQN avoids this risk by not needing to adjust the Q-function learned in the previous task.

7 Conclusion

We introduced boosted curriculum reinforcement learning (BCRL), a new method for action-value function estimation in curriculum RL. For each task, BCRL approximates the respective action-value function as a sum of residuals of the previous tasks in the curriculum. This procedure increases the representativeness of the functional space as the complexity of the tasks in the curriculum increases, instead of using a single approximator through all the learning. We proved that our BCRL method enjoys advantageous theoretical properties in terms of convergence to the optimal action-value function of the target task. Moreover, we empirically validated BCRL across different problems and algorithms, showing its overall advantages over regular curriculum RL.

REFERENCES

Chiye Aoki and Philip Siekevitz. Plasticity in brain development. *Scientific American*, 259(6):56, 1988.

Minoru Asada, Shoichi Noda, Sukoya Tawaratsumida, and Koh Hosoda. Purposive behavior acquisition for a real robot by vision-based reinforcement learning. *Machine learning*, 23(2):279–303, 1996.

Timur Ash. Dynamic node creation in backpropagation networks. *Connection science*, 1(4):365–375, 1989.

Yoshua Bengio, Jérôme Louradour, Ronan Collobert, and Jason Weston. Curriculum learning. *International Conference on Machine Learning*, 2009.

Steven J Bradtke. Reinforcement learning applied to linear quadratic regulation. In *Neural Information Processing Systems*, 1993.

Carlo D'Eramo, Davide Tateo, Andrea Bonarini, Marcello Restelli, and Jan Peters. Mushroomrl: Simplifying reinforcement learning research. *Journal of Machine Learning Research*, 22(131): 1–5, 2021.

Jeffrey L Elman. Learning and development in neural networks: The importance of starting small. *Cognition*, 48(1):71–99, 1993.

Thomas Elsken, Jan Hendrik Metzen, Frank Hutter, et al. Neural architecture search: A survey. *Journal of Machine Learning Research*, 20(55):1–21, 2019.

Damien Ernst, Pierre Geurts, and Louis Wehenkel. Tree-based batch mode reinforcement learning. *Journal of Machine Learning Research*, 6:503–556, 2005.

C Lebiere Fahlman. The cascade-correlation learning architecture. *Neural Information Processing Systems*, 1990.

Amir-massoud Farahmand. *Regularization in reinforcement learning*. PhD thesis, University of Alberta, 2011.

Amir Massoud Farahmand, Rémi Munos, and Csaba Szepesvári. Error propagation for approximate policy and value iteration. *Advances in Neural Information Processing Systems*, 2010.

Carlos Florensa, David Held, Markus Wulfmeier, Michael Zhang, and Pieter Abbeel. Reverse curriculum generation for reinforcement learning. *Conference on Robot Learning*, 2017.

Vincent François-Lavet, Peter Henderson, Riashat Islam, Marc G Bellemare, and Joelle Pineau. An introduction to deep reinforcement learning. *Foundations and Trends® in Machine Learning*, 11 (3-4):219–354, 2018.

Yoav Freund. Boosting a weak learning algorithm by majority. *Information and Computation*, 121 (2):256–285, 1995.

Pierre Geurts, Damien Ernst, and Louis Wehenkel. Extremely randomized trees. *Machine learning*, 63(1):3–42, 2006.

László Györfi, Michael Kohler, Adam Krzyzak, and Harro Walk. *A distribution-free theory of nonparametric regression*. Springer Science & Business Media, 2006.

Boris Ivanovic, James Harrison, Apoorva Sharma, Mo Chen, and Marco Pavone. Barc: Backward reachability curriculum for robotic reinforcement learning. *International Conference on Robotics and Automation*, 2019.

Lu Jiang, Deyu Meng, Qian Zhao, Shiguang Shan, and Alexander Hauptmann. Self-paced curriculum learning. *AAAI Conference on Artificial Intelligence*, 2015.

Pascal Klink, Carlo D'Eramo, Jan R Peters, and Joni Pajarinen. Self-paced deep reinforcement learning. *Advances in Neural Information Processing Systems*, 2020.

Kai A Krueger and Peter Dayan. Flexible shaping: How learning in small steps helps. *Cognition*, 110(3):380–394, 2009.

Michail G Lagoudakis and Ronald Parr. Least-squares policy iteration. *Journal of Machine Learning Research*, 4:1107–1149, 2003.

Jani JT Lahnajärvi, Mikko I Lehtokangas, and Jukka PP Saarinen. Evaluation of constructive neural networks with cascaded architectures. *Neurocomputing*, 48(1-4):573–607, 2002.

Volodymyr Mnih, Koray Kavukcuoglu, David Silver, Andrei A Rusu, Joel Veness, Marc G Bellemare, Alex Graves, Martin Riedmiller, Andreas K Fidjeland, Georg Ostrovski, et al. Human-level control through deep reinforcement learning. *Nature*, 518(7540):529–533, 2015.

Rémi Munos. Error bounds for approximate value iteration. *National Conference on Artificial Intelligence*, 2005.

Sanmit Narvekar, Bei Peng, Matteo Leonetti, Jivko Sinapov, Matthew E Taylor, and Peter Stone. Curriculum learning for reinforcement learning domains: A framework and survey. *Journal of Machine Learning Research*, 21(181):1–50, 2020.

Atsushi Nitanda and Taiji Suzuki. Functional gradient boosting based on residual network perception. *International Conference on Machine Learning*, 2018.

Martin L Puterman. Markov decision processes. *Handbooks in operations research and management science*, 2:331–434, 1990.

Françcois Rivest and Doina Precup. Combining td-learning with cascade-correlation networks. *International Conference on Machine Learning*, 2003.

David E Rumelhart, James L McClelland, PDP Research Group, et al. *Parallel distributed processing*, volume 1. IEEE Massachusetts, 1988.

J Saul, Leon. The behavior of organisms. an experimental analysis. *Psychoanalytic Quarterly*, 10: 164–166, 1941.

Robert E Schapire. The strength of weak learnability. *Machine learning*, 5(2):197–227, 1990.

Kun Shao, Yuanheng Zhu, and Dongbin Zhao. Starcraft micromanagement with reinforcement learning and curriculum transfer learning. *IEEE Transactions on Emerging Topics in Computational Intelligence*, 3(1):73–84, 2018.

Richard S Sutton and Andrew G Barto. *Reinforcement learning: An introduction*. MIT press, 2018.

Maxwell Svetlik, Matteo Leonetti, Jivko Sinapov, Rishi Shah, Nick Walker, and Peter Stone. Automatic curriculum graph generation for reinforcement learning agents. *AAAI Conference on Artificial Intelligence*, 2017.

Samuele Tosatto, Matteo Pirotta, Carlo D'Eramo, and Marcello Restelli. Boosted fitted q-iteration. *International Conference on Machine Learning*, 2017.

Peter Vamplew and Robert Ollington. Global versus local constructive function approximation for on-line reinforcement learning. *Australasian Joint Conference on Artificial Intelligence*, 2005a.

Peter Vamplew and Robert Ollington. On-line reinforcement learning using cascade constructive neural networks. *International Conference on Knowledge-Based and Intelligent Information and Engineering Systems*, 2005b.

Aad Van Der Vaart and Jon A Wellner. Preservation theorems for glivenko-cantelli and uniform glivenko-cantelli classes. In *High dimensional Probability II*, pp. 115–133. Springer, 2000.

A PROOFS

Theorem 2. *Let Q^*_{t-1} be the learned action-value for task $\mathcal{T}_{t-1}$, and $(Q^i_t)_{i=0}^k$ be a sequence of measurable action-value functions for a target task $\mathcal{T}_t$ obtained following our BCRL procedure (5), where $Q^0_t = Q^*_{t-1}$. Denote $L = \gamma C_{\mu\to\infty}$ the Lipschitz coefficient of the optimal Bellman operator, where $C_{\mu\to\infty}$ is the one-step concentrability coefficient w.r.t. μ (Farahmand, 2011), and assume the operator S is such that $\exists\lambda > 0 : \|(I-S)y\|_\mu \leq \lambda\|y\|_\mu$ for all $y \in \mathcal{B}(\mathcal{S}\times\mathcal{A})$. Then,*

$$\|Q^k_t - Q^*_t\|_\mu \leq ((1+L^k)\lambda + L^k)\|Q^0_t - Q^*_t\|_\mu. \tag{12}$$

Proof.

$$\begin{aligned}
\left\|Q^k_t - Q^*_t\right\|_\mu &\leq \left\|Q^k_t - (T^*_t)^k Q^0_t\right\|_\mu + \left\|(T^*_t)^k Q^0_t - Q^*_t\right\|_\mu \\
&= \left\|Q^{K_{t-1}}_{t-1} + S\varrho^k_t - (T^*_t)^k Q^0_t\right\|_\mu + \left\|(T^*_t)^k Q^0_t - Q^*_t\right\|_\mu \\
&\leq \lambda\left\|\varrho^k_t\right\|_\mu + L^k\left\|Q^0_t - Q^*_t\right\|_\mu \qquad (13)\\
&\leq \left(\lambda(1+L^k) + L^k\right)\left\|Q^0_t - Q^*_t\right\|_\mu. \qquad (14)
\end{aligned}$$

where (13) considers the assumption on the operator $(I-S)$ and (14) follows noting that

$$\begin{aligned}
\left\|\varrho^k_t\right\|_\mu &\leq \left\|(T^*_t)^k Q^0_t - T^*_t Q^*_t\right\|_\mu + \left\|T^*_t Q^*_t - Q^0_t\right\|_\mu \\
&\leq (1+L^k)\left\|Q^0_t - Q^*_t\right\|_\mu.
\end{aligned}$$

□

Theorem 3. *Let $(Q^i_t)_{i=0}^k$ be a sequence of action-value function for each task t, $(\varepsilon^i_t)_{i=0}^k$ be the respective sequence of approximation errors as defined in (8), $\mathcal{F} \subseteq \mathcal{B}(\mathcal{S}\times\mathcal{A})$ be a subset of measurable action-value functions. Denoting the regular AVI residual as $\bar{\varrho}^k_t = (T^*_t)^k \dots (T^*_1)^{K_1} Q^0_1 - (T^*_{t-1})^{K_{t-1}} \dots (T^*_1)^{K_1} Q^0_1$, we have*

$$\inf_{f\in\mathcal{F}} \|f - \varrho^k_t\|_\mu \leq \inf_{f\in\mathcal{F}} \|f - \bar{\varrho}^k_t\|_\mu + (1+L^k)\Big(\sum_{i=1}^{t-1} L^{K_i}\|\varepsilon^0_i\|_\mu + \|\varepsilon^0_t\|_\mu\Big). \tag{15}$$

Proof. For an arbitrary function $f \in \mathcal{F}$ and task t, we have $\|f - \varrho^k_t\|_\mu \leq \|f - \bar{\varrho}^k_t\|_\mu + \|\bar{\varrho}^k_t - \varrho^k_t\|_\mu$. Then,

$$\begin{aligned}
\left\|\bar{\varrho}^k_t - \varrho^k_t\right\|_\mu &\leq \left\|(T^*_t)^k \dots (T^*_1)^{K_1} Q^0_1 - (T^*_t)^k Q^0_t\right\|_\mu + \left\|(T^*_{t-1})^{K_{t-1}} \dots (T^*_1)^{K_1} Q^0_1 - Q^0_t\right\|_\mu \\
&\leq L^k\left\|(T^*_{t-1})^{K_{t-1}} \dots (T^*_1)^{K_1} Q^0_1 - Q^0_t\right\|_\mu + \left\|(T^*_{t-1})^{K_{t-1}} \dots (T^*_1)^{K_1} Q^0_1 - Q^0_t\right\|_\mu \\
&= (1+L^k)\left\|(T^*_{t-1})^{k_{t-1}} \dots (T^*_1)^{K_1} Q^0_1 - Q^0_t\right\|_\mu \\
&= (1+L^k)\left\|(T^*_{t-1})^{K_{t-1}} \dots (T^*_1)^{K_1} Q^0_1 - \left((T^*_{t-1})^{K_{t-1}} Q^0_{t-1} - \varepsilon^0_t\right)\right\|_\mu \\
&\leq (1+L^k)\Big(\left\|(T^*_{t-1})^{K_{t-1}} \dots (T^*_1)^{K_1} Q^0_1 - (T^*_{t-1})^{K_{t-1}} Q^0_{t-1}\right\|_\mu + \left\|\varepsilon^0_t\right\|_\mu\Big) \\
&\leq (1+L^k)\Big(L^{K_{t-1}}\left\|(T^*_{t-2})^{K_{t-2}} \dots (T^*_1)^{K_1} Q^0_1 - Q^0_{t-1}\right\|_\mu + \left\|\varepsilon^0_t\right\|_\mu\Big) \\
&\leq (1+L^k)\left(L^{K_{t-1}}\Big(\left\|(T^*_{t-2})^{K_{t-2}} \dots (T^*_1)^{K_1} Q^0_1 - (T^*_{t-2})^{K_{t-2}} Q^0_{t-2}\right\|_\mu + \left\|\varepsilon^0_{t-1}\right\|_\mu\Big) + \left\|\varepsilon^0_t\right\|_\mu\right) \\
&\leq \dots \leq (1+L^k)\Big(\sum_{i=1}^{t-1} L^{K_i}\left\|\varepsilon^0_i\right\|_\mu + \left\|\varepsilon^0_t\right\|_\mu\Big).
\end{aligned}$$

□

Theorem 4. *Let $B_k^t = \max(\|\tilde{\varrho}_t^k\|_\infty, 1)$, and $V_{\mathcal{F}^+}$ be the VC-dimension of $\mathcal{F}^+$, which is the class of all subgraphs of functions $f \in \mathcal{F}$ (Györfi et al., 2006). Given a dataset $\mathcal{D}_t = \{(s_t^i, a_t^i, r_t^i, s_t'^i)\}_{i=1}^N$ for each task t, and a sequence of action-value functions $(Q_t^i)_{i=0}^k$ generated by our BCRL, we have*

$$\|\varepsilon_t^k\|_\mu^2 \leq 2 \inf_{f \in \mathcal{F}} \|f - \bar{\varrho}_t^k\|_\mu^2 + 2(1+L^k)^2 \Big(\sum_{i=1}^{t-1} L^{K_i} \|\varepsilon_i^0\|_\mu + \|\varepsilon_t^0\|_\mu \Big)^2 + \frac{5136 B_t^{k^4}}{N} \Big(\log 42e + 2\log(480 e B_t^{k^2} N) V_{\mathcal{F}^+} \Big). \tag{16}$$

Proof. Using Theorem 5.11 from Györfi et al. (2006), we obtain

$$\|\varepsilon_t^k\|_\mu^2 \leq 2 \inf_{f \in \mathcal{F}} \|f - \varrho_t^k\|_\mu^2 + \frac{5136 B_t^{k^4}}{N} \Big(\log 42e + 2\log(480 e B_t^{k^2} N) V_{\mathcal{F}^+} \Big).$$

We complete the proof using (15) and the Cauchy-Schwartz inequality to bound the first term. □

Lemma 2. *Let $(Q_t^i)_{i=0}^k$ be a sequence of action-value function for each task t, $(\varepsilon_t^i)_{i=0}^k$ be the respective sequence of approximation errors as defined in (8). Then,*

$$\|\tilde{\varrho}_t^k\|_\infty \leq \sum_{i=1}^{k-1} \gamma^{k-i} \|\varepsilon_t^i\|_\infty + (1+\gamma^k) R_t^{\max}. \tag{17}$$

Proof. First, we bound the k-step Bellman residual.

Lemma 3. *Let $(Q_t^i)_{i=0}^k$ be a sequence of action-value function for each task t, $(\varepsilon_t^i)_{i=0}^k$ be the respective sequence of approximation errors as defined in (8). Then,*

$$\|\varrho_t^k\|_\infty \leq \sum_{i=1}^{k-1} \gamma^{k-i} \|\varepsilon_t^i\|_\infty + \gamma^k R_t^{\max}. \tag{18}$$

Proof.

$$\begin{aligned}
\|\varrho_t^k\|_\infty &= \|(T_t^*)^k Q_t^0 - Q_t^0\|_\infty \\
&= \sup_{s \in \mathcal{S}, a \in \mathcal{A}} \Big| r(s,a) + \gamma \int_{\mathcal{S}} \mathcal{P}(ds'|s,a) \max_{a' \in \mathcal{A}} Q_t^{k-1}(s',a') - Q_t^0(s,a) \Big| \\
&= \sup_{s \in \mathcal{S}, a \in \mathcal{A}} \Big| r(s,a) + \gamma \int_{\mathcal{S}} \mathcal{P}(ds'|s,a) \max_{a' \in \mathcal{A}} \big((T_t^*)^{k-1} Q_t^0(s',a') - \varepsilon_t^{k-1}(s',a') \big) - Q_t^0(s,a) \Big| \\
&\leq \gamma \|\varepsilon_t^{k-1}\|_\infty + \sup_{s \in \mathcal{S}, a \in \mathcal{A}} \Big| \gamma \int_{\mathcal{S}} \mathcal{P}(ds'|s,a) \Big(\max_{a' \in \mathcal{A}} (T_t^*)^{k-1} Q_t^0(s',a') - \max_{a'' \in \mathcal{A}} Q_t^0(s',a'') \Big) \Big| \\
&\leq \gamma \|\varepsilon_t^{k-1}\|_\infty + \gamma \sup_{s \in \mathcal{S}, a \in \mathcal{A}} \Big| \int_{\mathcal{S}} \mathcal{P}(ds'|s,a) \Big(\max_{a' \in \mathcal{A}} \big| (T_t^*)^{k-1} Q_t^0(s',a') - Q_t^0(s',a') \big| \Big) \Big| \\
&\leq \gamma \|\varepsilon_t^{k-1}\|_\infty + \gamma \|\varrho_t^{k-1}\|_\infty.
\end{aligned}$$

Since $\|\varrho_t^1\|_\infty \leq R_t^{\max}$, solving the recursion proves the lemma. □

We are now able to derive the bound for the k-step empirical Bellman residual.

$$\begin{aligned}
\|\tilde{\varrho}_t^k\|_\infty &= \|(\hat{T}_t^*)^k Q_t^0 - Q_t^0\|_\infty \\
&= \sup_{(s,a,r,s') \in \mathcal{D}_t} \Big| r + \gamma \max_{a' \in \mathcal{A}} Q_t^{k-1}(s',a') - Q_t^0(s,a) \Big| \\
&= \sup_{(s,a,r,s') \in \mathcal{D}_t} \Big| r + \gamma \max_{a' \in \mathcal{A}} \big((T_t^*)^{k-1} Q_t^0(s',a') - \varepsilon_t^{k-1}(s',a') \big) - Q_t^0(s,a) \Big| \\
&\leq \gamma \|\varepsilon_t^{k-1}\|_\infty + R_t^{\max} + \gamma \sup_{s'' \in \mathcal{S}} \max_{a' \in \mathcal{A}} \Big| (T_t^*)^{k-1} Q_t^0(s'',a') - Q_t^0(s'',a') \Big| \\
&\leq \gamma \|\varepsilon_t^{k-1}\|_\infty + R_t^{\max} + \gamma \|\varrho_t^{k-1}\|_\infty.
\end{aligned} \tag{19}$$

The bound is proved using (18). □

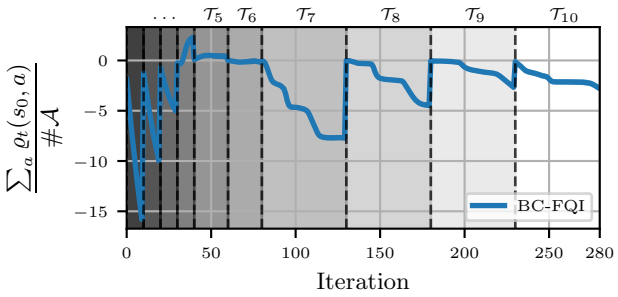

Figure 5: Average residual of the starting state $\mathbf{s}_0$ predicted by the learned Q-functions in the different learning tasks of the maze environment. The average and standard error (barely visible) is computed from 40 different seeds.

B Experimental Details

This section serves to present additional details on the experiments that did not fit in the main paper, such as algorithm hyperparameters and additional details of the learning environments. These additional details will be provided for each experiment individually in the following subsections. The computations were executed on a desktop computer with a Geforce RTX 2080, 64 GB memory and an AMD Ryzen 9 3900X processor. All experiments were run in roughly a week of computation time on this single machine. The employed MushroomRL library is available under the MIT license.

B.1 Car-on-hill

As mentioned in the main text, we used the FQI algorithm with extra-trees (Ernst et al., 2005) implemented in MushroomRL (D'Eramo et al., 2021) to conduct this experiment. The number of trees in the extra-trees implementation was set to 50, the minimum number of samples required to split an internal node to 5 and the minimum number of samples required to be a leaf node to 2. All other parameters were left to the implementation defaults of MushroomRL. Based on this implementation we created a boosted version that runs the original FQI algorithm on the residuals of the previously learned models. The hyperparameters for those extra-trees models were the same as for the regular FQI. The implementation can be found in the accompanying code. The car-on-hill environment used for this experiment is also implemented in MushroomRL.

B.2 Maze

The state space of the maze environments consists of the two-dimensional coordinates $\mathbf{s}=[s_x, s_y]\in[0,1]^2$. The initial state is $\mathbf{s}_0=[0,0]$, and the goal state is $\mathbf{g}_0=[0.95, 0.95]$. The four actions displace the agent in x- or y-position by a value of 0.05. The discount factor is set to γ=0.99 and the horizon length is 200. We use a dense reward function $\mathcal{R}(\cdot,\cdot,\mathbf{s}') = -|\mathbf{g}-\mathbf{s}'|$ when $|\mathbf{g}-\mathbf{s}'| >= 0.1$, otherwise $\mathcal{R}(\cdot,\cdot,\mathbf{s}') = +5$ and the episode terminates. There are two walls centered at $x = 0.2$ and $x = 0.6$, both with width w=0.05, and height h_t depending on the task t. We design a curriculum composed of 10 tasks, with $h_{1,\dots,9}$=$\{0.05, 0.15, \dots, 0.85\}$ and h_{10}=0.95. Hence in the final task $\mathcal{T}_{10}$, there is only a very narrow passage through which the walls can be passed.
We again make use of the FQI algorithm with extra-trees implemented in MushroomRL to conduct this experiment, again using 50 trees, a minimum number of 5 samples to split an internal node, a minimum number of 2 samples to be a leaf node and everything else left to the implementation defaults of MushroomRL. The main conceptual different to the car-on-hill experiment is that exploration is guided by the currently estimated Q-function, as we are employing an ε-greedy exploration strategy to generate the samples for learning the Q-functions of the learning tasks. The exploration percentage ε is annealed in later environments. More precisely, we set $\varepsilon_{1,\dots,10} = \{1., 1., 1., 1., .75, .75, .5, .5, .25, .25\}$ for the tasks $\mathcal{T}_1, \dots, \mathcal{T}_{10}$.
Figure 5 visualizes the residuals of the starting state $\mathbf{s}_0$ that the Q-functions learned in the individual tasks, i.e., the additional values the Q-functions needed to predict in addition to the Q-value predicted from the ensemble of previously learned Q-functions. We see that the magnitude of residuals continuously decreases from task $\mathcal{T}_1$ to task $\mathcal{T}_6$. Switching to task $\mathcal{T}_7$ increases the magnitude of the residuals after which it then continuously declines again. The reason for this jump is that, while the

optimal policy is largely unaffected by the presence of the small walls in the early learning tasks, a more significant detour is required starting from task $\mathcal{T}_7$.

B.3 LINEAR SYSTEM CONTROL

The linear system that needs to be controlled is given by

$$\dot{\mathbf{s}} = \begin{bmatrix} \dot{x} \\ \ddot{x} \\ \dot{y} \\ \ddot{y} \end{bmatrix} = \begin{bmatrix} 0 & 1 & 0 & 0 \\ 0 & -0.1 & 0 & 0 \\ 0 & 0 & 0 & 1 \\ 0 & 0 & 0 & -0.1 \end{bmatrix} \begin{bmatrix} x \\ \dot{x} \\ y \\ \dot{y} \end{bmatrix} + \begin{bmatrix} 0 & 0 \\ 1 & 0 \\ 0 & 0 \\ 0 & 1 \end{bmatrix} \begin{bmatrix} a_x \\ a_y \end{bmatrix} = \mathbf{A}\mathbf{s} + \mathbf{B}\mathbf{a},$$

representing a simple, fully-actuated point-mass with a slight amount of friction. For the LQR task, to which the curriculum learning agents are exposed first, the reward function is given by

$$r(\mathbf{s}, \mathbf{a}, \mathbf{s}') = -\mathbf{s}^T \begin{bmatrix} 3 & 0 & 0 & 0 \\ 0 & 1 & 0 & 0 \\ 0 & 0 & 3 & 0 \\ 0 & 0 & 0 & 1 \end{bmatrix} \mathbf{s} - \mathbf{a}^T \begin{bmatrix} 0.1 & 0 \\ 0 & 0.1 \end{bmatrix} \mathbf{a}$$

and the initial state is given by $\mathbf{s}_0 = [-4\ v_{x,0}\ 0\ v_{y,0}]^T$, where $v_{x,0}$ and $v_{y,0}$ are sampled uniformly within $[-0.3, 0.3]$. In the target task, the agent receives the following reward signal

$$r(\mathbf{s}, \mathbf{a}, \mathbf{s}') = \begin{cases} -1, \text{ if } \|[x\ y]^T\|_2 \geq 0.2 \\ 0, \text{ else} \end{cases}$$

and its initial position is given by $\mathbf{s}_0 = [-4\ v_{x,0}\ y\ v_{y,0}]^T$, where $v_{x,0}$ and $v_{y,0}$ are sampled uniformly within $[-0.1, 0.1]$ and y within $[-0.4, 0.4]$. Furthermore, the agent needs to keep its y-position within $[-0.5, 0.5]$ in order to stay on the pathway indicated in Figure 4b and it faces an additional drift moving it away from the target, particularly

$$\dot{\mathbf{s}} = \mathbf{A}\mathbf{s} + \mathbf{B}\mathbf{a} + \begin{bmatrix} -0.5 \\ 0 \\ 0 \\ 0 \end{bmatrix}.$$

Consequently, the policies pre-trained in the LQR do not quite reach the target but need to explore that they need to counteract this external force while staying on the pathway.
When learning with LSPI in the LQR system, we represent the policy by a PD-controller with explorative noise

$$\mathbf{a} \sim \mathcal{N}(\mathbf{K}\mathbf{s}, 0.1\mathbf{I})$$

as this ensures the quadratic form of the optimal Q-function mentioned in the main text (please see Bradtke (1993) for additional details). When learning with DQN in both the LQR and target task, the agent can choose between applying 8 discrete actions

$$a_1 = \begin{bmatrix} 1 \\ 0 \end{bmatrix},\ a_2 = \begin{bmatrix} 0 \\ 1 \end{bmatrix},\ a_3 = \begin{bmatrix} -1 \\ 0 \end{bmatrix},\ a_4 = \begin{bmatrix} 0 \\ -1 \end{bmatrix},$$
$$a_5 = \begin{bmatrix} .71 \\ .71 \end{bmatrix},\ a_6 = \begin{bmatrix} .71 \\ -.71 \end{bmatrix},\ a_7 = \begin{bmatrix} -.71 \\ .71 \end{bmatrix},\ a_8 = \begin{bmatrix} -.71 \\ -.71 \end{bmatrix}.$$

Consequently, we predict these discrete Q-values with the function approximator learned in the LQR task with LSPI when training on the target task. The Q-networks employed in DQN consist of two hidden layers of 128 neurons and ReLU activations. During training, we realized that the update frequency of the target network in the DQN algorithm had a strong impact on the final agent performance. Hence, we conducted a grid search testing values in $[25, 50, 100, 200, 500, 1000, 2000]$. For regular DQN on the target task, an update frequency of 200 performed best, while BC-DQN yielded best results with an update frequency of 2000. For C-DQN, best results where achieved when using an update frequency of 1000 in the LQR task and an update frequency of 25 in the target task. We used Adam for optimization of the network with a learning rate of 10^{-4} and $(\beta_1, \beta_2) = (0.9, 0.999)$. To exploit the previously learned policy in the target task for the curriculum methods, we used a fixed value of $\varepsilon = 0.1$ in the target task. For default DQN, we annealed ε from 1 to 0.1 over the first 1000 environment steps.